Current Imbalance Detection Method based on Vector Space Decomposition Approach for Five-Phase Induction Motor Drives

P. Salas-Biedma, I. Gonzalez-Prieto, M. J. Duran
Department of Electrical Engineering
E.I.I., Malaga University
29071 Malaga, Spain
psbiedma@uma.es, ignaciogp87@gmail.com, mjduran@uma.es

***Abstract*— The inherent fault-tolerant capability against open-phase faults (OPFs) of multiphase machines is an appreciated advantage in applications where high-reliability is a main concern. This desirable feature has usually required fault localization and post-fault control reconfiguration to provide a suitable performance in this anomaly situation. However, recent model predictive control (MPC) based on virtual voltage vectors (VVs) has validated the multiphase machine fault-tolerant capability without post-fault control reconfiguration. This fact allows to relax some of the OPF detection methods requirements. On the other hand, incipient faults or damaged connections can generate resistance dissymmetry (RD) situations that produces overheating and control degradation. Although the origin of OPFs and RDs can be of a different nature, the symptoms of both anomalies are common: a current imbalance that generates non-null x-y currents appears. Focusing on this approach, this work suggests new settings for an OPF detection method based on the vector space decomposition (VSD) in order to make it universally valid both in OPF and RD situations. The proposed current imbalance detection (CID) method is implemented together with a natural fault-tolerant direct torque control (DTC) for five-phase induction motor drives. Experimental results are employed to verify the goodness of the proposed method.**

Keywords—Fault detection method, resistance dissymmetry, natural fault tolerant, direct torque control (DTC), multiphase induction motor drives.

I. INTRODUCTION

The use of multiphase machines at industry has become a reality in the last decade with some emblematic applications using more than three phases in both motors and generators. [1-4]. The most relevant feature of multiphase drives is their inherent redundancy which enables a certain degree of fault tolerance without the use of additional hardware. Applications which require high power and reliability (such as aerospace, naval, or wind energy systems [5-7]) benefit from this characteristic.

Among different type of faults, the enhanced reliability against OPFs has been the most widely studied topic [8-13], requiring a mandatory fault detection (FD) stage. The requirements for an ideal FD method are typically assumed to be [12]:

R1. Fast detection.
R2. Ability to localize the fault.
R3. Use of non-invasive techniques.
R4. No need for additional hardware and/or high computational cost.
R5. Robustness against variation in the machine parameters, control strategies and operating conditions.

Although it is possible to inherit different three-phase FD methods that are available in literature, some recent proposals highlight the advantages of using specific multiphase FD methods that are based on the VSD. To name a few benefits, the VSD-FD methods provide a higher speed of detection, simplicity and robustness [12-13].

The FD stage has traditionally enabled a subsequent control reconfiguration stage according to the identified OPF scenario [14-16]. The modifications at the control stage are dependent on the control approach, with specific reconfiguration strategies for field-oriented control (FOC), direct torque control (DTC) or model predictive control (MPC). On the contrary, the VSD-FD methods are universally valid for all control approaches, thus fulfilling requirement R5. In spite of the good performance of the newly proposed VSD-FD methods [12-13], requirement R1 puts some strict constrains in the FD settings in order to avoid detection delays that eventually led to undesirable transients. Specifically, the dead-band of VSD-FD methods has to be mandatorily narrow and this limits the detection capability because only OPFs can be detected.

Nevertheless, there are other types of anomalies apart from OPFs that also require attention. Incipient faults or damaged connections can generate stator resistance RD and this phenomenon, in turn, produces a current imbalance that eventually led to overheating and control disturbance. From the point of view of the diagnosis, the detection of these current imbalance anomalies is important and requires a specific FD method. Unfortunately, the VSD-FD methods cannot be used to identify RD for two main reasons: the closed-loop control regulates the x-y currents closed to zero and need for a fast detection forces the FD method to focus on OPFs. Hence, some other methods for RD detection have been suggested in the literature of multiphase systems [17]. Nevertheless, requirement R5 is not fulfilled in [17] because the method is only valid for FOC and cannot be extended to methods lacking proportional-integer (PI) current controllers (e.g., DTC or MPC).

As a summary, three main facts can be highlighted:

i) VSD-FD methods successfully detect OPFs, but they do not serve to diagnose RDs.

ii) There are no RD detection methods for DTC or MPC strategies.

iii) There are no methods that simultaneously detect OPFs and RDs.

It must be highlighted however that fact *i)* is specifically conditioned by the use of a closed-loop x-y current control and by the need to reconfigure the control strategy after the

OPF. Fortunately, the latest findings demonstrate that it is possible to skip the control reconfiguration if virtual voltage vectors are used either in DTC or MPC strategies [18]. This key capability has been termed as natural or passive fault tolerance, and it can be achieved because the x-y current control is done in open-loop mode. The OPF still needs to be detected in order to apply the appropriate derating and safeguard the electric drive, but the fault detection delays will not affect the machine dynamics. Since the thermal time constant is much higher than its electrical counterpart, it follows that overcurrents will not affect the machine integrity in short time periods (i.e., in the range of a few electrical cycles). As far as the FD is concerned, the main implication of the natural fault tolerance is that requirement R1 is no longer critical. Consequently, the settings of the VSD-FD method from [12-13] can be relaxed with no practical impact on the transient from pre- to post-fault situation. Furthermore, the open-loop nature of the current control implies that x-y will be non-null in the event of RD and this opens the possibility to use VSD-FD methods for RD detection.

This work suggests new settings for the VSD-FD method it order to make it universally valid both in OPF and RD detection. Although the origin of OPFs and RDs can be of a different nature, the symptoms of both anomalies are common: a current imbalance that generates non-null x-y currents when x-y current control is done in open-loop mode. The modified version of the VSD-FD methods from [12-13] will then be referred to as a CID method. The CID becomes the first RD detection method that is valid for DTC and MPC, and at the same time, it can simultaneously detect OPFs with the use of single current imbalance indices. As a key feature, the CID serves both for diagnosis and fault tolerant purposes. The price to be paid is a slower FD, but fortunately this delay is fully admissible in multiphase drives with natural fault tolerance [18].

The CID method is tested in this paper together with a VV-DTC strategy (including VVs into the standard DTC scheme), but it can be extended to MPC or any control technique using VVs. The paper is organized as follows: section II describes generalities of five-phase induction machine (IM) drive in fault situation. Section III details the VSD-based CID method. Section IV presents the experimental rig and validates the goodness of the method with experimental results. Finally, section V summarizes the main conclusions obtained.

II. Five-Phase IM Drive in a Fault Operation

A. Topology Description

The drive topology under study consists of a five-phase IM supplied from a two-level five-phase insulated-gate bipolar transistor (IGBT)-based voltage source converter (VSC) that is powered by a single dc-link, as shown in Fig.1. The machine is built with distributed windings whose phases are symmetrically shifted 72 electrical degrees and linked to a single isolated neutral point.

B. Five-Phase IM Model

The multiphase machine behaviour can be expressed using a set of differential equations. These equations are usually expressed in phase variables, but they can also be expressed in other reference frames using different transformations. One of these transformations is the magnitude-invariant

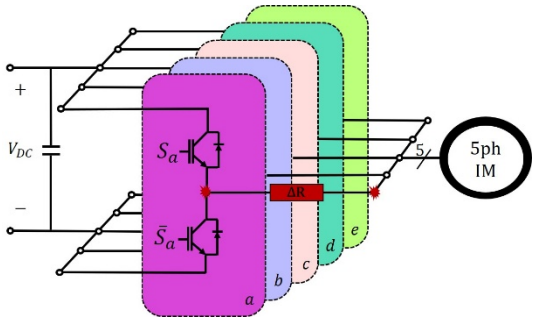

Fig. 1. Five-phase IM drive scheme in a RD operation.

generalized Clarke transformation (1) that provides the relationship between the phase and VSD variables (i.e., $\alpha\beta xy$) of the machine. Equation (1) will be employ in section III to define the fault indices.

$$[T] = \frac{2}{5}\begin{bmatrix} 1 & cos\theta & cos2\theta & cos3\theta & cos4\theta \\ 0 & sin\theta & sin2\theta & sin3\theta & sin4\theta \\ 1 & cos2\theta & cos4\theta & cos\theta & cos3\theta \\ 0 & sin2\theta & sin4\theta & sin\theta & sin3\theta \\ 1/2 & 1/2 & 1/2 & 1/2 & 1/2 \end{bmatrix} \quad (1)$$

$$[i_{\alpha s} \quad i_{\beta s} \quad i_{xs} \quad i_{ys} \quad i_{zs}]^T = [T][\, i_{as} \quad i_{bs} \quad i_{cs} \quad i_{ds} \quad i_{es}]^T$$

Since the machine is considered with distributed windings, only α-β current contribute to the flux and torque production. Conversely, the x-y currents only produce stator copper losses. Moreover, as the machine is configured with an isolated neutral point, the zero-sequence current (i_{zs}) cannot flow, and consequently this component can be omitted from the analysis. Applying standard assumptions, the VSD model of the five-phase IM can be expressed as:

$$\begin{aligned} v_{\alpha s} &= \left(R_s + L_s\frac{d}{dt}\right) i_{\alpha s} + M\frac{d}{dt} i_{\alpha r} \\ v_{\beta s} &= \left(R_s + L_s\frac{d}{dt}\right) i_{\beta s} + M\frac{d}{dt} i_{\beta r} \\ v_{xs} &= \left(R_s + L_{ls}\frac{d}{dt}\right) i_{xs} \\ v_{ys} &= \left(R_s + L_{ls}\frac{d}{dt}\right) i_{ys} \\ 0 &= \left(R_r + L_r\frac{d}{dt}\right) i_{\alpha r} + M\frac{d}{dt} i_{\alpha s} + \omega_r L_r i_{\beta r} + \omega_r M i_{\beta s} \\ 0 &= \left(R_r + L_r\frac{d}{dt}\right) i_{\beta r} + M\frac{d}{dt} i_{\beta s} - \omega_r L_r i_{\alpha r} - \omega_r M i_{\alpha s} \\ T_e &= \frac{5}{2} pM(i_{\beta r} i_{\alpha s} - i_{\alpha r} i_{\beta s}) \end{aligned} \quad (2)$$

where $L_s = L_{ls} + M$, $L_r = L_{lr} + M$, $M = 5/2\ L_m$, and $\omega_r = p\omega_m$, being p the pole pairs number and ω_m the mechanical speed. In addition, indices s and r denote stator and rotor variables and subscripts l and m denote leakage and magnetizing inductance, respectively.

C. Open phase fault and resistance dissymmetry in Five-Phase IM Drives

OPFs and RDs in IM drives can appear in different locations of the system: machine, VSC or connection between both [13,17]. Among different types of faults, OPF is the most widely studied topic due to the frequency of its occurrence [8-13]. When an OPF occurs in the proposed drive topology (regardless of its location), the current can no longer flow through the damaged phase. In order to achieve the same operation point, the current of the heathy phases have to increase, provoking an unavoidable current imbalance. From

the point of view of the control, the new restriction in the system due to the OPF occurrence (e.g., $i_{xs} = -i_{\alpha s}$ when OPF appears in phase a) cannot be deleted with any action of control and therefore this restriction can be defined as a hard constraint. Nevertheless, there are other types of anomalies (e.g., incipient faults or damaged connections) apart from OPFs that also require attention. RD is characterized by an increase of the stator resistance, which implies the current reduction through the damaged phase (and current increase in other phases). Regardless of the RD localization, this anomaly produces a current imbalance which can only be detected if the x-y currents of the machine are regulated in open-loop mode. Therefore, this restriction can be defined as a soft constraint.

As can be noted, both cases cause a certain degree of current imbalance and control disturbance. For this reason, the method described in this work searches for current imbalance of machine phases. However, not all kinds of dissymmetry should be treated as a fault. It is necessary to avoid the appearance of false alarms caused by measurement errors or unavoidable system asymmetries. If the phase current imbalance is kept below a certain threshold, it will be considered that the machine operates in regular mode. Otherwise, it can be affirmed that an OPF or RD take place in the machine. The aforementioned limits will be discussed in section III.

D. *Control Scheme*

Direct torque control based on virtual voltage vectors of [15] is employed in this work to regulate the multiphase drive (Fig. 2). This control is based on an outer PI-based speed control loop and two inner two-level stator flux and three-level electromechanical torque hysteresis comparators. The error signals $\Delta\lambda_s$ and ΔT_e and the stator flux position in the α-β subspace (ten different sectors are defined) are used to provide the suitable VV through a predefined look-up table. Stator flux is obtained using the observer detailed in [19] and torque is estimated as:

$$\hat{T}_e = 5/2\, p(\hat{\lambda}_{\alpha s} i_{\beta s} - \hat{\lambda}_{\beta s} i_{\alpha s}) \tag{3}$$

In this control, VVs are created to reduce harmonic currents in the x - y subspace, which do not produce torque/flux in a distributed-winding multiphase IM. Specifically, ten active VVs are defined in the α-β subspace for a five-phase IM, as it is shown in Fig. 3(b). These VVs are formed by couples of large and medium-large voltages vectors with the same direction in the α - β plane and opposite direction in the x-y plane. Moreover, in order to provide zero average voltage vector in the x - y subspace different application times are necessary (Fig. 3(a)):

$$VV_i = v_{large} K_{vl} + v_{medium} K_{vm} \tag{4}$$

where v_{large} and v_{medium} are two available voltage vectors aligned in the α - β subspace and $K_{\text{vl}} = (3 - \sqrt{5})/2$ and $K_{\text{vm}} = 1 - K_{vl}$ are normalized dwell times that are calculated to obtain zero average x-y voltages. With the implementation of VVs in a DTC scheme, the regulation of the x-y currents, is realized in open-loop mode. This fact provides the following two advantages: *i)* a natural fault tolerance is obtained due to elimination of the controllers' conflict in post-fault situation [18] and *ii)* dissymmetry faults can be detected using x-y currents, since in this situation null x-y voltages can no longer produce null x-y currents and therefore there are currents imbalance.

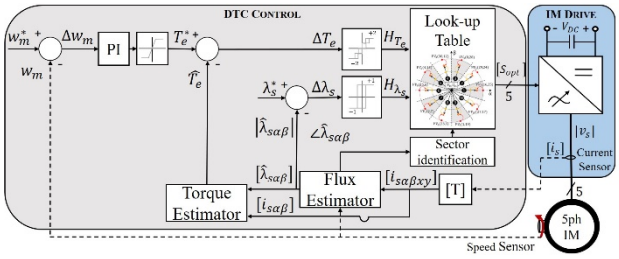

Fig. 2. VV-DTC scheme for the five-phase IM drive. The "^" and " $*$ " symbols identify the estimated and reference variables, respectively.

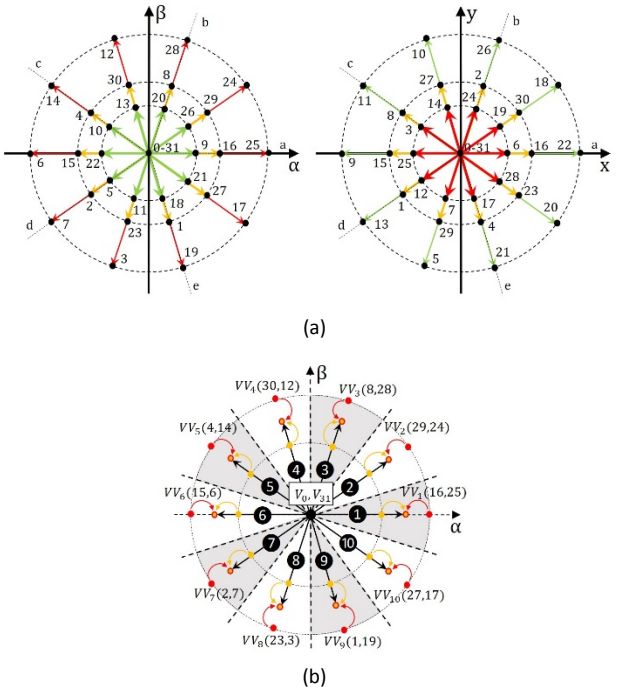

Fig. 3. (a) The upper figure shows available voltage vectors in the α-β subspace (left plot) and x-y subspace (right plot) for a five-phase IM. (b) Virtual voltage vectors (VV_i) in the α-β subspace for a five-phase IM.

III. Description of the Proposed Current Imbalance Detection Method

This section describes the different stages of the proposed CID method based on the VSD variables. The aim of CID method is: *i)* to locate the damaged phase and *ii)* to classify the type of fault.

A. *Current imbalance indices*

The procedure to obtain the VSD-based current imbalance indices is to use the inverse Clarke transformation defined in (1) and set the most restrictive situation, an OPF ($i_{phase} = 0$). Then extract from this restriction the corresponding index. For the sake of example, when phase a is under OPF, the restriction is $-i_{xs}/i_{\alpha s} = 1$, which leads to the following current imbalance index: $CI_a = -i_{xs}/i_{\alpha s}$. The process can be generalized for the remaining phases, whose indices can be obtained as [13]:

$$
\begin{aligned}
CI_a &= -\frac{i_{xs}}{i_{\alpha s}} \\
CI_b &= \frac{i_{xs}}{0.38i_{\alpha s} + 1.71i_{\beta s} - 0.73i_{ys}} \\
CI_c &= \frac{i_{xs}}{2.62i_{\alpha s} - 1.90i_{\beta s} + 3.08i_{ys}} \\
CI_d &= \frac{i_{xs}}{2.62i_{\alpha s} + 1.90i_{\beta s} - 3.08i_{ys}} \\
CI_e &= \frac{i_{xs}}{0.38i_{\alpha s} - 1.17i_{\beta s} - 0.73i_{ys}}
\end{aligned} \tag{5}
$$

The current imbalance indices from (5) differ as a function of number of phases and the spatial shift between the windings. However, the procedure for determine the fault indices is the same and it can consequently be extended to any multiphase machine. If the one phase current is suddenly decreased, the index of that phase will rise. If the index goes beyond a certain threshold (0.2 in this work to avoid false alarms), this will mean that a significant RD exists. Meanwhile, healthy phases indices will still have a close to zero value.

B. Dead-band

The method then applies a dead-band to the indices CI_k for noise rejection. Sinusoidal feature of α-β currents leads to zero value of indices denominator causing the indices sometimes achieve high values. Moreover, it ensures a low ripple of healthy phases indices. This dead-band was set in [12] in between 0.9 and 1.1 because the theoretical value of the index under OPF is 1. This narrow dead-band was necessary in order to allow a rather short integration period (see next subsection) and speed-up in this manner the fault detection process. However, this specific setting makes the RD detection impossible. Since the VV-DTC from Fig. 2 provides a natural fault tolerance, it is possible to enlarge the dead-band in order to also detect resistance dissymmetries. Specifically, the dead-band is set in the range 0.2 to 1.1 so that is covers RDs (in the range 0.2 to 0.9) and OPFs (in the range 0.9 to 1.1), as schematically shown in Fig. 4.

$$
CI_k^{db} = \begin{cases} CI_k, \ if \ CI_k \in [0.2, 1.1] \\ 0, \ otherwise \end{cases} \quad k \in \{a, b, c, d, e\} \tag{6}
$$

C. Moving window average

The CID method cannot be applied using instantaneous values because zero crossings might be regarded as OPFs, hence leading to false alarms. An alternative is to integrate indices over a period T_m:

$$
FR_k(t) = \frac{1}{T_m} \int_{t-T_m}^{t} CI_k^{db}(\tau)\, d\tau, \qquad k \in \{a, b, c, d, e\} \tag{7}
$$

The integration period T_m does not need to be equal to the electrical period T_f. In fact, it can be chosen as a fraction of it to accelerate the detection [12-13]. It must be highlighted that the lower this parameter is the higher ripple it has, but the faster detection it provides. Thus, a trade-off between these two characteristics will be found to obtain a satisfactory value for T_m.

$$
T_m = \sigma \cdot T_f, \qquad \sigma \geq 0 \tag{8}
$$

While σ was set to 0.66 in [12-13] because the speed of detection was critical, the VV-DTC does not need any reconfiguration after the OPF. Consequently, the integration period T_m can be set to a much higher value. In this work σ is set to 5 in order to reduce the ripple of the fault indices in the whole range (i.e., from $0.2\ to\ 1.1$). It is worth highlighting that setting σ to 5 provides enough speed of detection both for RD diagnosis and for the application of the derating in OPF operation.

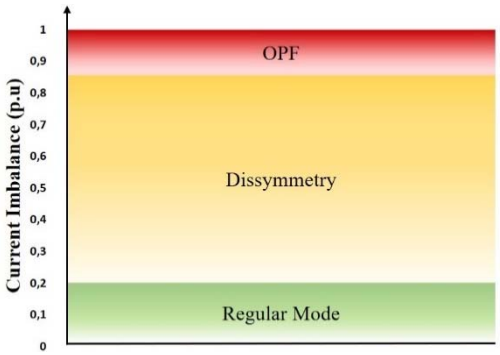

Fig. 4. Limits of the CID method.

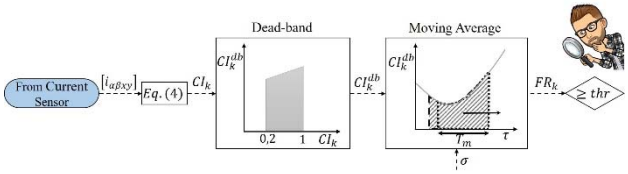

Fig. 5. CID method scheme.

D. Threshold

Once fault indices are defined (FR_k), a proper threshold must be established to avoid false alarms caused by measurement errors or unavoidable system asymmetries. FR_k are not null even when no type of fault occurs (9). A RD threshold (0.2) and OPF threshold (0.85) value have been chosen after testing several degrees of RD and OPFs respectively (Fig. 4).

$$
FR_k \neq 0, \qquad \forall\ k \in \{a, b, c, d, e\} \tag{9}
$$

To summarize, the basic stages of the CID method are: A) define current imbalance indices, B) filter them with a dead-band, C) determine a suitable moving window and D) define the threshold for the detection. While the CID procedure (Fig. 5) is the same as for the VSD-FD methods for OPFs [12,13], the settings for the dead-band, the integration period and the thresholds have been modified to allow the detection of both OPFs and RDs with a single method. The new settings can be used together with any control method using open-loop x-y current control. The next section will confirm the validity of the new setting to make the CID method universally valid for all king of current imbalances.

IV. Experimental Results

The aim of this section is to verify that the VSD-based CID method can successfully locate and classify any type of current imbalance. The proposed method is tested with VV-DTC-based five-phase induction motor drive in three situations: A) OPF, B) RD and C) transient tests. In the first two tests, the machine is driven at 500 rpm with no load.

A scheme of the utilized experimental system is shown in Fig.6. It is based on a five-phase IM drive fed by a five-phase VSC. The control is implemented in an electronic board based on the MSK28335 using a sampling period of $100\ \mu s$. A programmable load torque can be applied using a DC machine

mechanically coupled to the five-phase IM, while the DC-link voltage is set using an external DC supply to 300 V. The parameters of the custom-built five-phase machine (Table I) have been determined with ac-time domain and stand-still tests [20], [21].

A. OPF

Two tests have been performed: test 1 for a single OPF in phase a (see Fig. 7) and test 2 for dual OPFs in phases a and b at $t = 1s$ (see Fig. 8). These two different situations were selected to notice that in the first case, the current imbalance index of damaged phase only involves $i_{\alpha s}$ and i_{xs}, while all VSD variables are implicated in the second case (5).

In both tests, OPFs occur (all the switches from one phase are forced to keep current out) when the multiphase drive reaches the steady state. An OPF is characterized by zero phase current once the fault has happened (see the zoom-in left subplots in Fig. 7 and Fig. 8). For this reason, the new restriction appears with the fault occurrence, leads to a non-null xy currents (see the zoom-in right subplots in Fig. 7 and Fig. 8). Consequently, the fault indices of the faulty phases quickly rise while the rest of indices remain close to zero.

B. RD

Two tests have been performed in steady state: test 3 for a 50% (see Fig. 9) and test 4 for a 20% (see Fig. 10) of current imbalance in phase a. These two validate the capability of the proposed method to detect and localize different degrees of resistance dissymmetry. Therefore, a reduction of the phase current occurs (see zoom-in left subplots in Fig. 9 and Fig. 10) and non-null xy currents appear (see zoom-in right subplots in Fig. 9 and Fig. 10). As the percentage of current imbalance increases, xy currents differ from zero value. The most restrictive case has been discussed in test 1 when an OPF appears and $i_{xs} = -i_{\alpha s}$ is fulfilled. Please note that a RD situation is only considered when fault ratios surpass the threshold value (20% of current imbalance).

C. Transient test

It is necessary to prove that the proposed method is robust against transients and avoids false alarms. For this purpose, a transient test has been carried out. It consists of a speed reduction at $t = 0.5s$, from 500 rpm to 350 rpm without load torque, as shown in Fig. 11. Despite the phase current reduction due to transient speed, fault ratios are maintained close to zero without false alarms in the system. This fact implies that the suggested method is not sensitive to dynamic changes in the machine.

V. Conclusion

Among several anomalies that can be present in the operation of a multiphase drive, OPFs and RD have a significant importance and require detection. It is found however that there are no specific multiphase RD diagnosis methods when proportional-integer (PI) current controllers do not exist. Furthermore, a universal current CID method that simultaneously distinguishes between OPFs and RDs does not exist in literature.

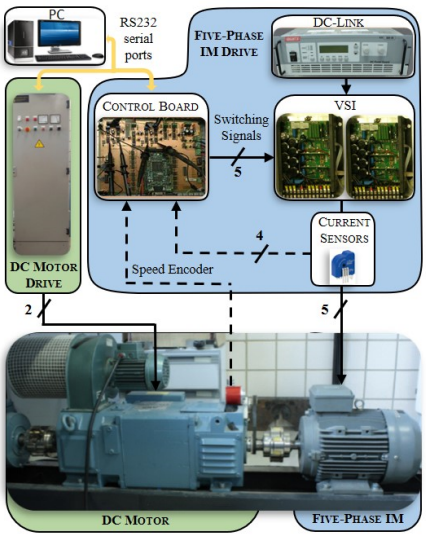

Fig. 6. Scheme of the test bench.

TABLE I
Induction Motor Parameters and Rated values

Power (kW)	0.7
DC-link voltage (V)	300
Torque $(N \cdot m)$	6.27
$n_m\ (rpm)$	1000
$I_{peak}\ (A)$	3.8
$R_s\ (\Omega)$	12.85
$R_r\ (\Omega)$	4.80
$L_m\ (mH)$	681.70
$L_{ls}\ (mH)$	79.93
$L_{lr}\ (mH)$	79.93

When the control is reconfigured after the OPF occurrence, the need for a fast FD makes the RD detection unfeasible. Fortunately, the recent natural fault-tolerant approach allows a somewhat slower FD and this opens the possibility to relax the CID settings. This work demonstrates that enlarging the dead-band and integration period and setting new thresholds, it is possible to: *i)* locate the damaged phase and *ii)* classify the type of fault (either OPF or RD), using a single CID method in a five-phase drive regulated with a VV-DTC strategy. Experimental results are employed to verify that the proposed method is robust against transients with fault indices that are maintained close to zero without false alarms in the system.

References

[1] E. Levi, F. Barrero and M.J. Duran, "Multiphase machines and drives – Revisited," *IEEE Trans. Ind. Electron*., vol. 63, no. 1, pp. 429-432, Jan. 2016.

[2] E. Levi, "Advances in converter control and innovative exploitation of additional degrees of freedom for multiphase machines," *IEEE Trans. Ind. Electron*., vol. 63, no. 1, pp. 433-448, 2016.

[3] F. Barrero and M. J. Duran, "Recent advances in the design, modeling and control of multiphase machines – Part I," *IEEE Trans. Ind. Electron*., vol. 63, no. 1, pp. 449-458, 2016.

[4] M. J. Duran and F. Barrero, "Recent advances in the design, modeling and control of multiphase machines – Part II," *IEEE Trans. Ind. Electron*., vol. 63, no. 1, pp. 459-468, 2016.

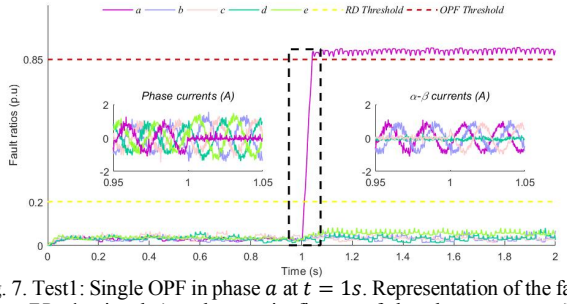

Fig. 7. Test1: Single OPF in phase a at $t = 1s$. Representation of the fault ratios FR_k (main plot) and zoom-in figures of the phase currents (left subplot) and α-β currents (right plot).

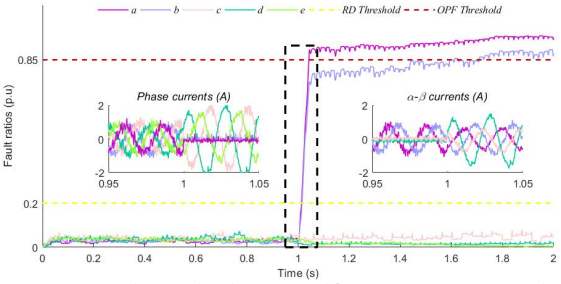

Fig. 8. Test 2: Dual OPFs in phases a and b at $t = 1s$. Representation of the fault ratios FR_k (main subplot) and zoom-in figures of the phase currents (left subplot) and α-β currents (right subplot).

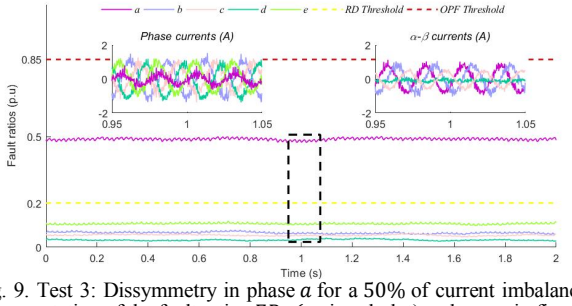

Fig. 9. Test 3: Dissymmetry in phase a for a 50% of current imbalance. Representation of the fault ratios FR_k (main subplot) and zoom-in figures of the phase currents (left subplot) and α-β currents (right subplot).

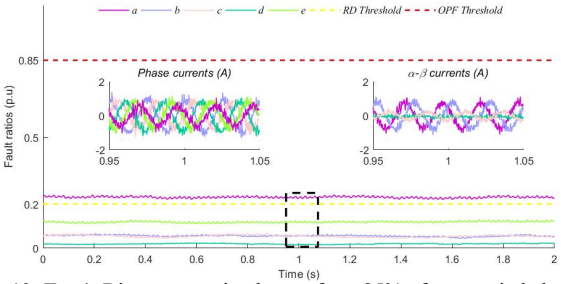

Fig. 10. Test4: Dissymmetry in phase a for a 25% of current imbalance. Representation of the fault ratios FR_k (main subplot) and zoom-in figures of the phase currents (left subplot) and α-β currents (right subplot).

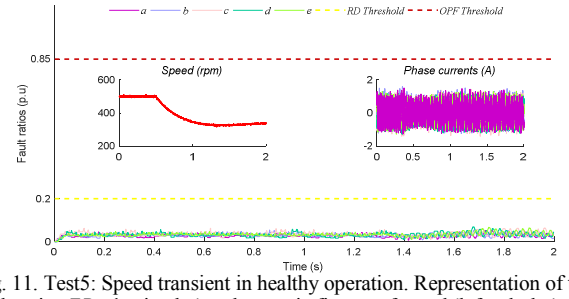

Fig. 11. Test5: Speed transient in healthy operation. Representation of the fault ratios FR_k (main plot) and zoom-in figures of speed (left subplot) and phase currents (right subplot).

[5] E. Jung, H. Yoo, S. Sul, H. Choi, and Y. Choi, "A nine-phase permanentmagnet motor drive system for an ultrahigh-speed elevator," *IEEE Trans. Ind. Appl*., vol. 48, no. 3, pp. 987-995, May/Jun. 2012.

[6] V. Yaramasu, A. Dekka, M. J. Duran, S. Kouro, and B. Wu, "Permanent magnet synchronous generator-based wind energy conversion systems: Survey on power converters and controls," *IET Elect. Power Appl.*, vol. 11, no. 6, pp. 956-968, 2017.

[7] A. Cavagnino, Z. Li, A. Tenconi, and S. Vaschetto, "Integrated generator for more electric engine: Design and testing of a scaled-size prototype," *IEEE Trans. Ind. Appl*., vol. 49, no. 5, pp. 2034-2043, Sep./Oct. 2013

[8] H.Henao, G. A. Capolino, M. Fernandez-Cabanas, F. Filippetti, C. Bruzzese, E. Strangas, R. Pusca, J. Estima, M. Riera-Guasp and S. Hedayati-kia, "Trends in Fault Diagnosis for Electrical Machines: A review of Diagnostic Techniques," *IEEE Ind. Electron. Magazine.,* vol. 8, no. 2, pp. 31-42, 2014.

[9] M. Riera-Guasp, J. A. Antonino-Daviu, and G. A. Capolino, "Advances in Electrical Machine, Power electronic, and Drive Condition Monitoring and Fault Detection: State of the Art" *IEEE Trans. On Ind. Electron.,* vol. 62, no. 3, pp. 1746-1759, 2015.

[10] J. O. Estima and A. J. M. Cardoso, "A new approach for real-time multiple open-circuit fault diagnosis in voltage source inverters," *IEEE Trans. Ind. Applicat.,* vol. 47, no. 6, pp. 2487-2494, 2011.

[11] N. M. A. freire, J. O. Estima, and A. J. M. Cardoso, "Open-circuit fault diagnosis in PMSG drives for wind turbine applications," *IEEE Trans. Ind. Electron.,* vol. 60, no. 9, pp. 3957-3967, 2013.

[12] M. J. Duran, I. Gonzalez-Prieto, N. Rios and F. Barrero, "A simple, fast and robust open-phase fault detection technique for six-phase induction motor drives" *IEEE Trans. On Power Electron.,* vol. 33, no. 1, pp. 547-557, Jan. 2018.

[13] I. Gonzalez-Prieto, M. J. Duran, N. Rios, F. Barrero and Cristina Martín, "Open-Switch Fault Detection in Five-Phase Induction Motor Drives Using Model Predictive Control," *IEEE Trans. Ind. Electron*., vol. 65, no. 4, pp. 3045-3055, Apr. 2018.

[14] H. Guzman, M.J.Duran, F. Barrero, L. Zarri, B. Bogado, I. Gonzalez-Prieto, M.R. Arahal, "Comparative Study of Predictive and Resonant Controllers in Fault-Tolerant Five-Phase Induction Motor Drives," *IEEE Trans. Ind. Electron.,* vol. 63, no. 1, pp. 606-617, Jan. 2016.

[15] M. Bermudez, I. Gonzalez-Prieto, F. Barrero, H. Guzman, X. Kestelyn and M. J. Duran, "An Experimental Assessment of Open-Phase Fault-Tolerant Virtual-Vector-Based Direct Torque Control in Five-Phase Induction Motor Drives," *IEEE Trans. On Power Electronics*. vol. 33, no. 3, pp. 2774-2784, March. 2018.

[16] M. Bermudez, I. Gonzalez-Prieto, F. Barrero, H. Guzman, M. J. Duran, and X. Kestelyn, "Open-phase fault-tolerant direct torque control technique for five-phase induction motor drives," *IEEE Trans. Ind. Electron*., vol. 61, no. 9, pp. 4474-4484, Sep. 2014.

[17] L. Zarri, M. Mengoni, Y. Griti, A. Tani, F. Filippetti, G. Serra and D. Casadei, "Detection and localization of stator resistance dissymmetry based on multiple reference frame controllers in multiphase induction motor drives," *IEEE Trans. Ind. Electron*., vol. 60, no. 8, pp. 3506-3518, 2013.

[18] I. Gonzalez-Prieto, M. J. Duran, M. Bermúdez, F. Barrero and C. Martín, "Assessment of Virtual-Voltage-based Model Predictive Controllers in Six-phase Drives under Open-Phase Faults," *IEEE Journal of Emerging and Selected Topics in Power Electronics.,* to be published., doi:*10.1109/JESTPE.2019.2915666.*

[19] J. A. Riveros, F. Barrero, E. Levi, M. Duran, S. Toral, and M. Jones, "Variable-speed five-phase induction motor drive based on predictive torque control," *IEEE Trans. Ind. Electron*., vol. 60, no. 8, pp. 2957-2968, Aug. 2013.

[20] A. Yepes *et al*., "Parameter identification of multiphase induction machines with distributed windings - Part 1: Sinusoidal excitation methods," *IEEE Trans. Energy Convers*., vol. 27, no. 4, pp. 1056-1066, Dec. 2012.

[21] J. A. Riveros et al., "Parameter identification of multiphase induction machines with distributed windings - Part 2: time-domain techniques," *IEEE Trans. Energy Convers.*, vol. 27, no. 4, pp. 1067-1077, Dec. 2012.